

Identification of circ_0058357 as a regulator in non-small cell lung cancer cells resistant to cisplatin by miR-361-3p/ABCC1 axis

Dan Chu¹ | Pengpeng Li² | Yameng Li¹ | Jiang Shi¹ | Siyuan Huang¹ | Pengfei Jiao¹ 

¹Department of Respiratory Medicine, the First Affiliated Hospital of Zhengzhou University, Zhengzhou, China

²Cancer Gamma Knife Center, the Fifth Affiliated Hospital of Zhengzhou University, Zhengzhou, China

Correspondence

Pengfei Jiao, Department of Respiratory Medicine, the First Affiliated Hospital of Zhengzhou University, No. 1 Jianshe East Road, Zhengzhou, 450052, China.
Email: fccjiaopf@zzu.edu.cn

Abstract

Background: Drug resistance is a major clinical drawback behind the failure of chemotherapy in non-small cell lung cancer (NSCLC). In this study, we undertook to identify the precise role of circular RNA (circRNA) circ_0058357 in the functional properties of DDP-resistant NSCLC cells.

Methods: Circ_0058357, miR-361-3p and ATP-binding cassette (ABC) subfamily C member 1 (ABCC1) were quantified by qRT-PCR and western blot. Cell survival and viability were gauged by MTT assay. Cell proliferation, apoptosis, invasion and migration were measured by EdU, flow cytometry, transwell and wound-healing assays, respectively. The direct relationship between miR-361-3p and circ_0058357 or ABCC1 was validated by dual-luciferase reporter assay.

Results: Our data showed that circ_0058357 was highly expressed in DDP-resistant NSCLC tissues and cells. Inhibition of circ_0058357 repressed cell growth, invasion, migration, and promoted DDP sensitivity and cell apoptosis of H1299/DDP and A549/DDP cells in vitro. Moreover, inhibition of circ_0058357 diminished the growth of A549/DDP cells and sensitized them to the cytotoxic effect of DDP in vivo. Mechanistically, circ_0058357 contained a miR-361-3p binding site and miR-361-3p was identified as a molecular mediator of circ_0058357 regulation. MiR-361-3p suppressed ABCC1 expression by binding to ABCC1 3'UTR, and miR-361-3p-mediated inhibition of ABCC1 affected the growth, invasion, migration, apoptosis and DDP sensitivity of H1299/DDP and A549/DDP cells. Furthermore, circ_0058357 regulated ABCC1 expression by competitively binding to shared miR-361-3p.

Conclusions: Our findings identified that inhibition of circ_0058357 suppresses the growth and metastasis of H1299/DDP and A549/DDP cells and sensitizes them to DDP therapy partially by targeting the miR-361-3p/ABCC1 axis.

KEYWORDS

ABCC1, chemoresistance, circ_0058357, miR-361-3p, NSCLC

INTRODUCTION

Non-small cell lung cancer (NSCLC), accounting for the majority of lung cancer, is one of the biggest causes of cancer mortality worldwide.¹ Cisplatin (DDP) is a clinically used chemotherapeutic drug and DDP-based therapy has been the standard-of-care for NSCLC patients, with a good performance status.^{2,3} Unfortunately, DDP resistance frequently

arises, giving rise to a major clinical drawback. Despite intensive efforts, mechanisms of resistance to DDP are still not fully understood. Thus, to develop novel therapeutic approaches to improve DDP efficacy in NSCLC, identifying the mechanisms of DDP resistance is required.

Circular RNAs (circRNAs), a new kind of noncoding RNAs, are covalently closed RNA transcripts with neither 5' caps nor 3' tails.⁴ Numerous studies have unveiled the

post-transcriptional regulation of circRNAs in gene expression by competitively binding to shared microRNAs (miRNAs), highlighting the importance of such interactions in cancer pathogenesis and drug resistance.^{5–7} Moreover, abnormal expression of circRNAs in DDP-resistant NSCLC cells has been reported.⁸ For instance, Lu et al.⁹ uncovered that circ_0096157 could regulate the malignant behaviors of DDP-resistant A549 cells (A549/DDP). Pang et al.¹⁰ ascertained that downregulation of circ_0031250 restrained the growth and invasion of A549/DDP and H460/DDP cells and sensitized them to DDP therapy depending on the modulation of the miR-4458/REV3L axis. Zhong et al.¹¹ demonstrated that circ_100565 was able to affect the functional properties, including DDP sensitivity, in DDP-resistant NSCLC cell lines by binding to miR-337-3p to induce ADAM metallopeptidase domain 28. Circ_0058357, formed by the head-to-tail splicing of exons of autophagy related 9A (ATG9A) transcript, has been identified as a potent tumor driver in NSCLC by upregulating AVL9 cell migration associated (AVL9) by competing for shared miR-24-3p.¹² In the preliminary survey, we found that circ_0058357 is differentially expressed in DDP-resistant NSCLC (A549/DDP) cells versus the sensitive parental cells (Figure S1). Herein, we undertook to explore the precise action of circ_0058357 in the functional properties of DDP-resistant NSCLC cells.

Deregulated expression of miRNAs in DDP-resistant NSCLC cells has also been uncovered.¹³ Recent studies have identified the antitumor role of miR-361-3p in NSCLC,^{14–16} suggesting its tremendous therapeutic potential in NSCLC. Moreover, downregulation of miR-361-3p is reported to be associated with gefitinib resistance in NSCLC.¹⁷ ATP-binding cassette (ABC) subfamily C member 1 (ABCC1, multidrug resistance-associated protein 1/MRP1) is a pivotal player in cancer-related multidrug resistance.¹⁸ Furthermore, resistance of NSCLC to DDP involves ABCC1, wherein ABCC1 operates as a contributor to resistance development.^{19–21} Here, we provide evidence that circ_0058357, an overexpressed circRNA in DDP-resistant NSCLC, affects the functional properties and DDP sensitivity of A549/DDP and DDP-resistant H1299 (H1299/DDP) NSCLC cells. We also identify circ_0058357 as a post-transcriptional regulator of ABCC1 expression through miR-361-3p, highlighting a novel circRNA/miRNA/mRNA network in DDP-resistant NSCLC cells.

METHODS

Human samples and cell lines

We obtained all human NSCLC samples from the First Affiliated Hospital of Zhengzhou University with written informed consent provided by all subjects. Use of human samples was approved by the Ethics Committee of the First Affiliated Hospital of Zhengzhou University. In total, we analyzed 21 primary tumors (defined as sensitive) collected from NSCLC primary patients before therapeutic treatment

and 23 NSCLC tissues (defined as resistant) obtained from recurrent patients after treatment of DDP-based chemotherapy to evaluate the expression levels of circ_0058357, miR-361-3p and ABCC1.

We obtained human bronchial epithelial cells (HBE), A549, H1299, H1299/DDP and A549/DDP NSCLC cells from Procell. All cells were propagated in 10% FBS RPMI-1640 medium (PAA-Laboratories) containing 1% streptomycin–penicillin (Life Technologies) at 5% CO₂, 85% humidity at 37°C.

RNA preparation, ribonuclease R (RNase R) treatment and quantitative real-time PCR (qRT-PCR)

We prepared total RNA using the NucleoSpin RNA II from tissue samples and cultured cells as recommended by the manufacturers (Macherey-Nagel). We isolated the cytoplasmic and nuclear RNA using the cytoplasmic and nuclear RNA purification kit from H1299/DDP and A549/DDP cells based on the manufacturer's protocols (Norgen Biotek). RNase R treatment was performed by adding 5 U of RNase R (Geneseed) into 2 µg total RNA and 10 min incubation at 37°C.

For the quantification of circ_0058357 and mRNAs, reverse transcription (RT) PCR generated cDNA was done using the random hexamers with QuantiTect RT Kit (Qiagen); amplification of gene-specific products was achieved by qRT-PCR using SYBR Green (Qiagen) and designed primers (Table S1). For miRNA analysis, RT PCR was done using the stem-loop RT primers and miScript II RT Kit (Qiagen) and cDNA products were amplified and quantified with miRNA-specific primers (Table S1) and miScript SYBR Green Kit as per the manufacturer's recommendations. Using the comparative Ct method ($2^{-\Delta\Delta C_t}$), we determined the relative expression of target genes relative to the housekeeping gene β -actin or U6.

Plasmids, oligonucleotides, and transient transfection of cells

Human circ_0058357 expression plasmid pCD5-circ_0058357 and control plasmid pCD5-ciR were purchased from Geneseed. Human ABCC1 expression plasmid was constructed by inserting human ABCC1 coding sequence (lacking the 3'UTR), synthesized by AbioCenter into EcoR I and Xba I sites of the pcDNA3.1 vector (YouBio). Circ_0058357 siRNA (si-circ_0058357) and mock siRNA (si-NC), miR-361-3p mimic and mock mimic (miR-NC), anti-miR-361-3p and anti-miR-NC oligo were obtained from GenePharma and their sequences are shown in Table S1.

We plated H1299/DDP and A549/DDP cells in 12-well dishes at 2×10^5 cells per well. The next day, the cells were transfected with 30 nM miRNA mimic, 30 nM miRNA inhibitor, or 100 nM siRNA and RNAiMAX or 1 µg of

plasmid DNA and lipofectamine 3000 as per the manufacturer's recommendations (Invitrogen) for transfection. We harvested the transfected cells for cell viability, proliferation, migration, invasion assays after 12 h and for apoptosis and expression analyses after 72 h.

MTT assay for cell survival and viability

The transfected H1299/DDP and A549/DDP cells were seeded in 96-well dishes at 3000 cells per well and cultured at 37°C for 48 h. The cells were then challenged with (survival analysis) or without (viability analysis) various concentrations of DDP (Sigma-Aldrich) for 24 h. The medium was replaced by fresh growth media containing 0.5 mg/ml of MTT solution (Roche). Following a 4-h incubation at 37°C, DMSO was used to dissolve formazan crystal. The number of viable cells was proportional to the optical density measured by a PowerWave340 reader (BioTek Instruments). We estimated the IC₅₀ value of DDP from a plot of the percentage (50%) of viable cells versus DDP concentration.

Cell proliferation and apoptosis assays

We evaluated cell proliferation with the 5-ethynyl-2'-deoxyuridine (EdU) assay and cell apoptosis using flow cytometry. For proliferation analysis, the transfected H1299/DDP and A549/DDP cells were seeded in 96-well dishes at 3000 cells per well and cultured at 37°C for 48 h. After that, cells were orderly incubated with 50 μM of EdU solution (Invitrogen) for 2 h, Apollo488 staining solution (Ribobio) and 4',6-diamidino-2-phenylindole (DAPI, Invitrogen) nuclear staining solution for 20 min. Fluorescence microscopy was performed in 10 random fields with a fluorescence microscope (Leica). The ratio of EdU-positive nuclei (green) to total nuclei (blue) was calculated as the proliferation rate of transfected cells. For apoptosis analysis, the transfected H1299/DDP and A549/DDP cells were stained using a Roche Annexin V-FITC/propidium iodide (PI) staining kit as recommended by the manufacturers (Roche). Stained cells were analyzed with a MUSE Cell Analyzer (Merck Millipore). We considered the cells that were positive for Annexin V as the apoptotic cells.

Measuring cell invasion by transwell assay

We plated the transfected H1299/DDP and A549/DDP cells at 2×10^5 cells per well into 24-well transwell inserts pre-coated with Matrigel (8 μm pore size, Corning). We placed the inserts into the culture dishes containing the fresh growth media. Following a 24-h culture at 37°C (cell proliferation was not significantly inhibited by circ_0058357 silencing in this time point (Figure S2), the invaded cells (5 randomly selected fields per sample) on the undersurface

of the membrane were counted using 100× bright-field microscopy with a microscope (Nikon).

Measuring cell migration by wound-healing assay

The transfected H1299/DDP and A549/DDP cells were seeded into six-well dishes and cultured at 37°C for 6 h to create a monolayer. Subsequently, a homogeneous wound track was made using the tip of a fine forceps. We acquired images at 0 and 24 h of at least five randomly selected microscopic fields and quantified cell migration by analyzing the area of wound repair with NIS Elements software (Nikon).

Western blot

We obtained total protein from tissue samples and cultured cells using the RIPA buffer (Merck Millipore) supplemented with protease inhibitors (Thermo Fisher Scientific) as per the accompanying recommendations. For immunoblotting, proteins were resolved on the Mini-Protean TGX gels (Bio-Rad) by electrophoresis, and the resulting gels were electrotransferred to nitrocellulose membranes (Bio-Rad). The primary antibodies (Abcam) employed were: rabbit monoclonal CyclinD1 (ab16663), rabbit monoclonal ABCC1 (ab260038), rabbit polyclonal matrix metalloproteinase 9 (MMP9, ab38898), rabbit polyclonal multidrug resistance 1 (MDR1, ab129453) and rabbit monoclonal GAPDH (ab181602). The anti-rabbit IgG labeled by HRP was used as the secondary antibody (ab205718, Abcam). Immunoreactivity was detected by ECL (Merck Millipore), and band densitometry was analyzed with the ChemiDoc MP Imager and Image Lab software as described by the manufacturers (Bio-Rad).

Bioinformatics

To search the miRNA-binding sites to circ_0058357, we used the StarBase and Circinterctome computational algorithms. We also used the StarBase target prediction software to predict the molecular targets of miR-361-3p.

Dual-luciferase reporter assay

The segment of circ_0058357 or ABCC1 3'UTR harboring the predicted miR-361-3p complementary sites, provided by Abiocenter, was cloned into Xho I and Pme I sites downstream of the SV40 promoter-driven renilla luciferase cassette in psiCHECK-2 vector (Promega). Mutations in the seed sequence were generated by TaKaRa MutanBEST Kit as described by the manufacturers (TaKaRa). MiR-361-3p mimic (30 nM) or negative control and the indicated reporter construct (200 ng) were cotransfected into

H1299/DDP and A549/DDP cells using lipofectamine 3000. We tested the luciferase activity after 48 h using the dual-luciferase reporter system with a luminometer based on the manufacturer's guidance (Promega).

Generation of stable circ_0058357 depletion cell line

We obtained lentiviral particles coding circ_0058357 shRNA (sh-circ_0058357) or mock shRNA (sh-NC) from Geneseeed. A stable circ_0058357 depletion cell line was achieved by transducing the virus particles into A549/DDP cells in media containing 8 µg/ml polybrene. Two days after infection, virus-positive cells were selected with puromycin (2 µg/ml) for 2 weeks.

Xenograft model studies

All animal experiments followed international guidelines and the study was approved by the Animal Care and Use Committee of the First Affiliated Hospital of Zhengzhou University. We used 6–8-week-old BALB/c female nude mice (Ai Ling Fei Biotechnology Co., Ltd.) for examining the effect of circ_0058357 on the tumorigenicity of A549/DDP cells and DDP cytotoxic activity. For xenograft formation, we gave BALB/c nude mice a 200 µl volume of PBS containing 4×10^6 transduced A549/DDP cells by subcutaneous injection into their right flanks. After eight days, we performed DDP (30 mg/kg, every 3 days) or PBS administration by intraperitoneal injection and measured tumor volumes ($\text{length} \times \text{width}^2/2$) using a digital caliper every three days. Each group included six mice. On day 23, mice were sacrificed by CO₂ overdose according to institutional ethics guidelines. Postmortem examination included weight measurement, and the tumors were analyzed for circ_0058357, miR-361-3p, ABCC1 and MMP9 expression levels by qRT-PCR and western blot as above and immunohistochemistry assay with antibodies against ABCC1 (ab260038, Abcam) and MMP9 (MA5-15886, Invitrogen), as described elsewhere.²²

Statistical analysis

Data are presented as means of at least three independent experiments performed in quintuplicate, with the standard error of the mean. In general, we used a two-tailed Student's *t*-test (two groups) or analysis of variance with Dunnett's post hoc test (multiple groups) to compare significant differences. We employed the Pearson's correlation coefficients to analyze the expression correlation between miR-361-3p and circ_0058357 or ABCC1 in NSCLC tissues obtained from recurrent patients after treatment of DDP-based chemotherapy. Values of $p < 0.05$ were considered statistically significant.

RESULTS

Overexpression of circ_0058357 in DDP-resistant NSCLC

To observe the relevance of circ_0058357 in adaptive DDP resistance, we initially examined its expression pattern by qRT-PCR analysis and found a clear upregulation of circ_0058357 in a panel of DDP-resistant NSCLC tissues compared with the primary sensitive NSCLC tumors (Figure 1(a)). We also assessed circ_0058357 expression in H1299/DDP and A549/DDP NSCLC cells. H1299/DDP and A549/DDP cells showed increased expression of circ_0058357 compared to the parental cells (Figure 1(b)). Additionally, we performed RNase R treatment to validate the RNase R resistance of circ_0058357. Circ_0058357 was more tolerant of RNase R digestion than the linear GAPDH transcript (Figure 1(c),(d)), suggesting that circ_0058357 has a higher tolerance to exonucleases. Moreover, subcellular localization analysis revealed that circ_0058357 predominantly localized to the cytoplasm of H1299/DDP and A549/DDP cells (Figure 1(e),(f)).

Inhibition of circ_0058357 impedes cell growth, invasion, migration, and promotes DDP sensitivity and cell apoptosis of H1299/DDP and A549/DDP cells in vitro

To elucidate the precise role of circ_0058357, we decreased circ_0058357 expression with siRNA-targeting circ_0058357 (si-circ_0058357) in H1299/DDP and A549/DDP cells, which expressed high levels of circ_0058357. The circ_0058357 inhibition efficacy of si-circ_0058357 was verified by qRT-PCR analysis (Figure 2(a)). H1299/DDP and A549/DDP cells exhibited higher IC₅₀ values of DDP compared with the sensitive parents (Figure 2(b)). Intriguingly, circ_0058357 loss of function markedly lessened the IC₅₀ for DDP of H1299/DDP and A549/DDP cells (Figure 2(c)), indicating that inhibition of circ_0058357 sensitized H1299/DDP and A549/DDP cells to DDP therapy. Moreover, downregulation of circ_0058357 potentially hindered the viability (Figure 2(d)) and proliferation (Figure 2(e)) of H1299/DDP and A549/DDP cells. Conversely, downregulation of circ_0058357 strongly enhanced cell apoptosis of H1299/DDP and A549/DDP cells compared with the si-NC controls (Figure 2(f)). Furthermore, circ_0058357-silenced H1299/DDP and A549/DDP cells showed suppressed invasion (Figure 2(g)) and migration (Figure 2(h)) rates compared to the controls. Additionally, inhibition of circ_0058357 resulted in decreased levels of cycle-related cyclin D1, migration-related MMP9 and MDR1 in H1299/DDP and A549/DDP cells compared with the si-NC controls (Figure 2(i),(j)). Together, these findings establish that circ_0058357 affects cell functional properties and DDP sensitivity of H1299/DDP and A549/DDP cells.

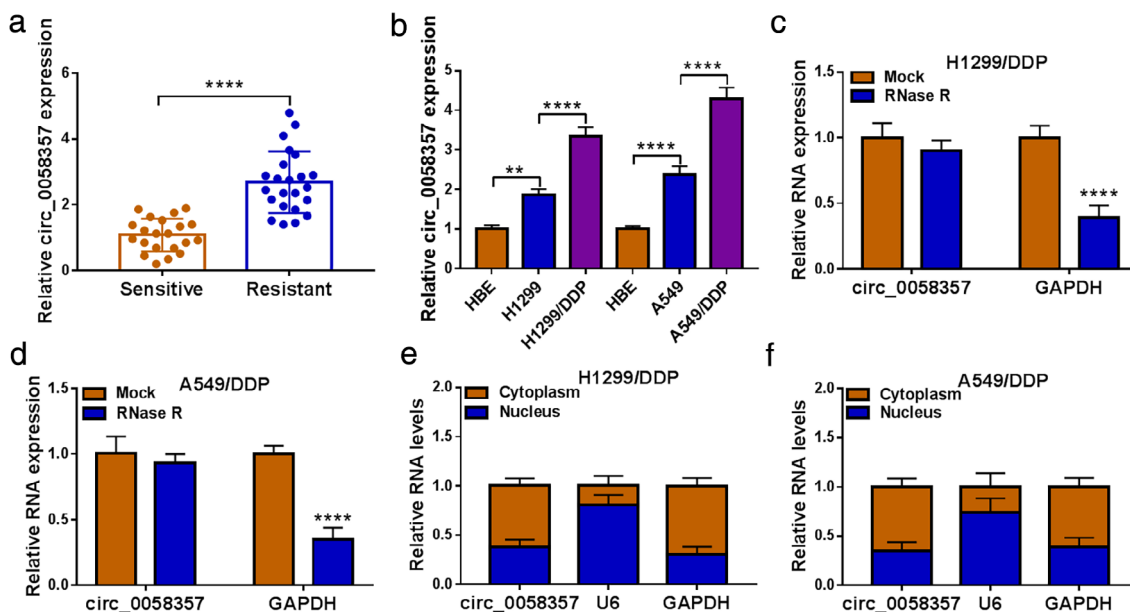


FIGURE 1 Overexpression of circ_0058357 in DDP-resistant NSCLC. (a) qRT-PCR analysis of circ_0058357 in clinical NSCLC tissues from 23 recurrent patients after treatment of DDP-based chemotherapy (Resistant) and 21 primary patients before therapeutic treatment (Sensitive). (b) Relative circ_0058357 expression in A549/DDP, A549, H1299/DDP, H1299 NSCLC cells and human normal HBE cells by qRT-PCR analysis. (c) and (d) RNase R resistance of circ_0058357 was validated by RNase R treatment. (e) and (f) The main cytoplasmic localization of circ_0058357 was confirmed by subcellular localization analysis. $^{**}p < 0.01$, $^{****}p < 0.0001$

MiR-361-3p is a crucial mediator of circ_0058357 regulation

To understand how circ_0058357 influences the functional properties of H1299/DDP and A549/DDP cells, we considered its targeted miRNAs as the potential downstream mediators of circ_0058357 function. Using the StarBase and Circinteractome computational algorithms, we found that there existed five miRNAs (miR-532-3p, miR-503, miR-545-3p, miR-665 and miR-361-3p) that overlapped by the two methods (Figure 3(a)). Intriguingly, we observed the significant upregulation of miR-545-3p and miR-361-3p in circ_0058357-silenced H1299/DDP and A549/DDP cells (Figure 3(b),(c)). Of them, miR-361-3p was the most significantly upregulated as a result of circ_0058357 depletion ($p < 0.0001$, Figure 3(b),(c)). We thus selected miR-361-3p for further studies. Bioinformatic analysis by the StarBase method revealed that circ_0058357 harbored a putative complementary region for miR-361-3p (Figure 3(d)). Analysis of miR-361-3p expression in DDP-resistant NSCLC tissues showed that miR-361-3p was markedly suppressed in DDP-resistant NSCLC tissues compared with the sensitive controls (Figure 3(e)). Having established that inhibition of circ_0058357 elevated miR-361-3p expression (Figure 3(b), (c)), we asked if there existed an inverse correlation between miR-361-3p and circ_0058357 levels in DDP-resistant NSCLC tissues. As expected, miR-361-3p expression inversely correlated with circ_0058357 level in NSCLC tissues from recurrent patients (Figure 3(f)). Furthermore, H1299/DDP and A549/DDP cells showed lower expression

of miR-361-3p compared with the matched sensitive cells (Figure 3(g)). To ascertain the direct relationship between circ_0058357 and miR-361-3p, we cloned the circ_0058357 fragment containing the predicted target sequence into a luciferase vector and mutated the miR-361-3p target sequence. The effectiveness of miR-361-3p mimic transfection in elevating miR-361-3p was verified by qRT-PCR analysis (Figure 3(h)). With the wild-type reporter and miR-361-3p upregulation produced a clear downregulation in luciferase activity (Figure 3(i),(j)). When the target sequence was mutated, little decrease was observed with miR-361-3p elevation (Figure 3(i),(j)). Additionally, overexpression of circ_0058357 by an expression plasmid introduction, confirmed by qRT-PCR (Figure 3(k)), caused a distinct repression in the level of endogenous miR-361-3p in H1299/DDP and A549/DDP cells (Figure 3(l)).

On the basis of our findings that circ_0058357 could affect miR-361-3p expression, we hypothesized that the effects of circ_0058357 deficiency are due to the elevation of miR-361-3p. To address this possibility, we decreased miR-361-3p expression with miRNA inhibitor (anti-miR-361-3p) in circ_0058357-silenced H1299/DDP and A549/DDP cells (Figure 4(a)). Remarkably, downregulation of miR-361-3p reversed circ_0058357 depletion-caused reduction of the IC₅₀ for DDP of H1299/DDP and A549/DDP cells (Figure 4(b)). Moreover, downregulation of miR-361-3p strongly abrogated circ_0058357 loss-driven anti-invasion (Figure 4(c)), anti-proliferation (Figure 4(d)), proapoptosis (Figure 4(e)), anti-invasion (Figure 4(f)), and anti-migration (Figure 4(g)) effects in H1299/DDP and A549/DDP cells. Furthermore,

reduced expression of miR-361-3p strikingly counteracted the impact of circ_0058357 depletion on CyclinD1, MMP9 and MDR1 expression levels in H1299/DDP and A549/DDP

cells (Figure 4(h),(i)). All these results suggest that inhibition of circ_0058357 affects the functional properties of H1299/DDP and A549/DDP cells partially through miR-361-3p.

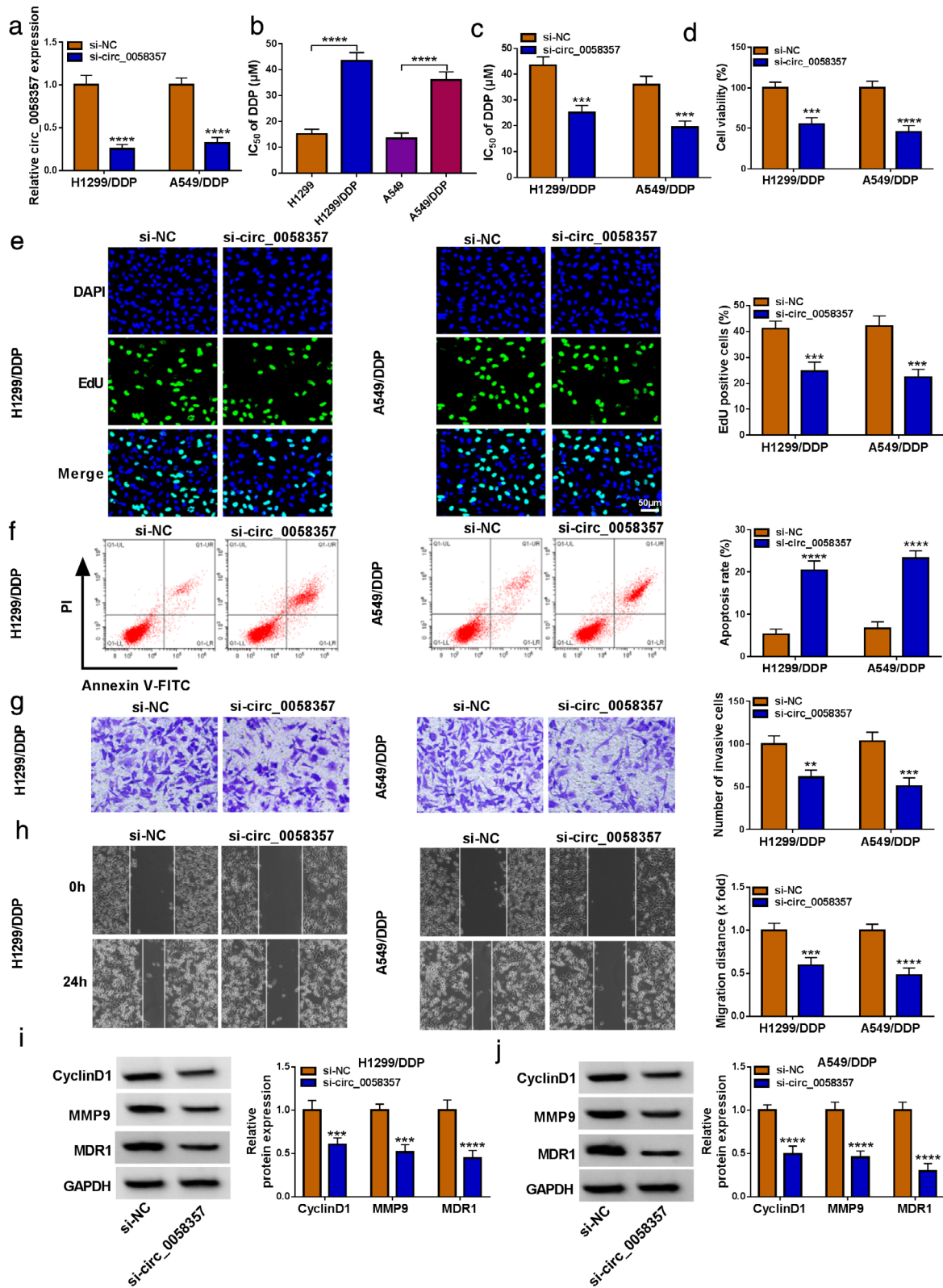


FIGURE 2 Legend on next page.

ABCC1 is a direct target of miR-361-3p

To identify the downstream effectors of miR-361-3p, we used the computational target prediction StarBase. Intriguingly, we found that the 3'UTR of ABCC1 harbored a putative binding region for miR-361-3p (Figure 5(a)). In both H1299/DDP and A549/DDP cell lines, introduction of miR-361-3p mimic reduced the luciferase activity of the wild-type 3'UTR reporter construct, not the mutant-type 3'UTR reporter (Figure 5(b), (c)). Additionally, in DDP-resistant NSCLC tissues, ABCC1 was highly expressed and it inversely correlated with miR-361-3p level (Figure 5(d)–(f)). Moreover, ABCC1 protein level

was significantly upregulated in H1299/DDP and A549/DDP cells compared with the sensitive controls (Figure 5(g)). The ability of miR-361-3p to regulate the endogenous ABCC1 protein was also tested. H1299/DDP and A549/DDP cells were transfected with miR-361-3p mimic or anti-miR-361-3p. The miR-361-3p reduction efficacy of anti-miR-361-3p was evaluated by qRT-PCR analysis (Figure 5(h)). As would be expected, ABCC1 protein level was decreased by miR-361-3p overexpression, and conversely elevated by reduced expression of miR-361-3p (Figure 5(i)). Taken together, these findings demonstrate that miR-361-3p regulates ABCC1 expression through the perfect binding sequence in ABCC1 3'UTR.

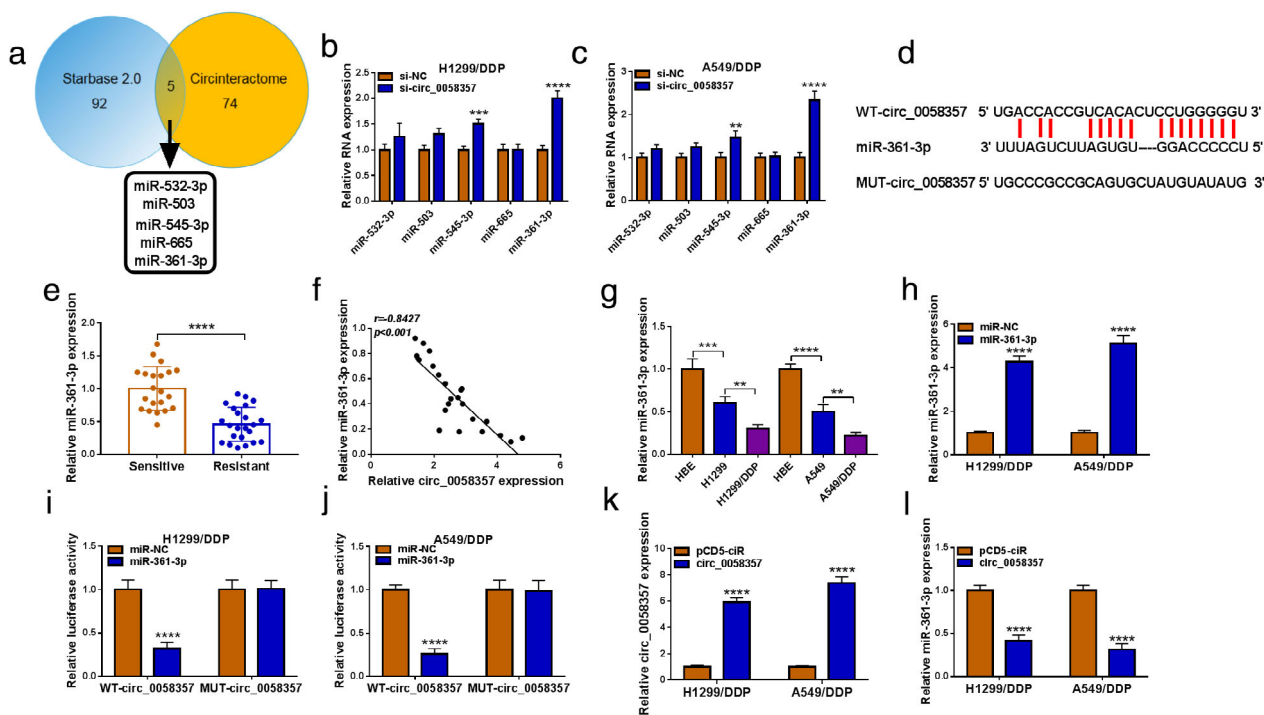


FIGURE 3 Circ_0058357 targets miR-361-3p. (a) Venn diagrams showing the putative target miRNAs of circ_0058357 predicted by the Starbase and Circinteractome computational algorithms. (b) and (c) qRT-PCR analysis of miR-532-3p, miR-503, miR-545-3p, miR-665 and miR-361-3p expression in si-circ_0058357- or si-NC-transfected H1299/DDP and A549/DDP cells. (d) Sequence of miR-361-3p, the putative miR-361-3p complementary sequence within circ_0058357 and the mutation in the target sequence. (e) qRT-PCR analysis of miR-361-3p expression in clinical NSCLC tissues from 23 recurrent patients after treatment of DDP-based chemotherapy (Resistant) and 21 primary patients before therapeutic treatment (Sensitive). (f) Expression correlation between miR-361-3p and circ_0058357 in NSCLC tissues from 23 recurrent patients after treatment of DDP-based chemotherapy (Resistant). (g) Relative expression of miR-361-3p in A549/DDP, A549, H1299/DDP, H1299 NSCLC cells and human normal HBE cells was gauged by qRT-PCR analysis. (h) The expression of miR-361-3p in miR-361-3p mimic- or miR-NC mimic-transfected H1299/DDP and A549/DDP cells was gauged by qRT-PCR analysis. (i) and (j) Dual-luciferase reporter assays revealing the suppression of miR-361-3p on luciferase activity of WT-circ_0058357 but not MUT-circ_0058357. qRT-PCR analysis of circ_0058357 (k) and miR-361-3p (l) expression in H1299/DDP and A549/DDP cells transfected with circ_0058357 expression plasmid or pCD5-ciR control plasmid. ** $p < 0.01$, *** $p < 0.001$, **** $p < 0.0001$

FIGURE 2 Circ_0058357 regulates the growth, invasion, migration, apoptosis and DDP sensitivity of H1299/DDP and A549/DDP cells in vitro. (a) qRT-PCR analysis of circ_0058357 in si-circ_0058357- or si-NC-transfected H1299/DDP and A549/DDP cells. (b) MTT assay presenting the IC₅₀ for DDP in A549/DDP, A549, H1299/DDP, H1299 NSCLC cells. (c) H1299/DDP and A549/DDP cells were introduced with si-circ_0058357 or si-NC and exposed to various concentrations of DDP for 24 h, followed by the evaluation of the IC₅₀ of DDP by MTT assay. (d)–(j) H1299/DDP and A549/DDP cells were introduced with si-circ_0058357 or si-NC for 48 h. (d) The viability of transfected H1299/DDP and A549/DDP cells was examined by MTT assay. (e) Representative images depicting a cell proliferation assay performed by the usage of EdU assay. (f) Representative pictures displaying a cell apoptosis assay performed by flow cytometry. (g) Representative images showing a cell invasion assay and transwell assay for cell invasion. (h) Representative pictures depicting a cell migration assay and cell migration by wound-healing assay. (i) and (j) The levels of CyclinD1, MMP9 and MDR1 in transfected H1299/DDP and A549/DDP cells were detected by western blot. ** $p < 0.01$, *** $p < 0.001$, **** $p < 0.0001$

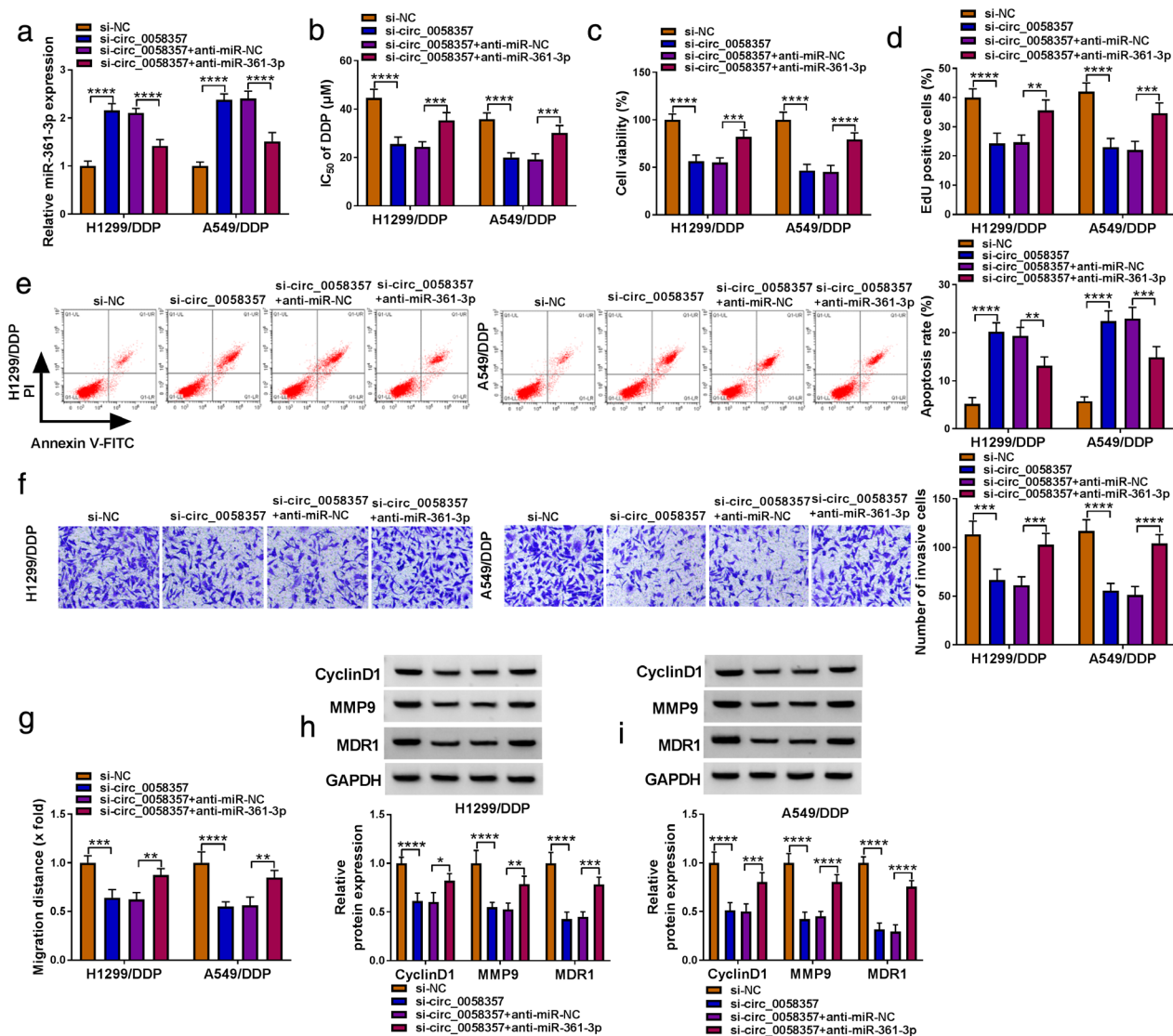


FIGURE 4 The effects of circ_0058357 inhibition are abolished by the downregulation of miR-361-3p. (a)–(i) H1299/DDP and A549/DDP cells were transfected with si-circ_0058357 + anti-miR-361-3p, si-circ_0058357 + anti-miR-NC, si-circ_0058357 or si-NC. (a) qRT-PCR analysis of miR-361-3p expression in transfected H1299/DDP and A549/DDP cells. (b) Transfected H1299/DDP and A549/DDP cells were exposed to various concentrations of DDP and checked for cell survival and the IC₅₀ value by MTT assay. (c) The viability of transfected H1299/DDP and A549/DDP cells by MTT assay. (d) The proliferation of transfected H1299/DDP and A549/DDP cells by EdU assay. (e) Flow cytometry of cell apoptosis of transfected H1299/DDP and A549/DDP cells. (f) Transwell assay of cell invasion of transfected H1299/DDP and A549/DDP cells. (g) Wound-healing assay of cell migration of transfected H1299/DDP and A549/DDP cells. (h) and (i) Western blot showing CyclinD1, MMP9 and MDR1 levels in transfected H1299/DDP and A549/DDP cells. **p* < 0.05, ***p* < 0.01, ****p* < 0.001, *****p* < 0.0001

MiR-361-3p-mediated inhibition of ABCC1 regulates the growth, invasion, migration, apoptosis and DDP sensitivity of H1299/DDP and A549/DDP cells

Apart from the inhibition of ABCC1 expression (Figure 6(a)), enforced expression of miR-361-3p by miR-361-3p mimic introduction reduced the IC₅₀ of DDP (Figure 6(b)), suppressed cell viability (Figure 6(c)), proliferation (Figure 6(d)), as well as accelerated cell apoptosis (Figure 6(e)), and hampered cell invasion (Figure 6(f)) and migration (Figure 6(g)) of H1299/DDP and A549/DDP cells. Enforced expression of miR-361-3p also decreased the protein levels of

cyclin D1, MMP9 and MDR1 in both H1299/DDP and A549/DDP cell lines (Figure 6(h),(i)).

To elucidate whether ABCC1 is a downstream effector of miR-361-3p function, we overexpressed miR-361-3p in H1299/DDP and A549/DDP cells together with a recombinant plasmid expressing ABCC1; this plasmid encodes the ABCC1 coding sequence but lacks the 3'UTR, yielding an mRNA that is resistant to miR-361-3p-driven inhibition of translation. The effectiveness of the recombinant plasmid in increasing ABCC1 protein level was validated by western blot (Figure 6(a)). Notably, restoration of ABCC1 protein abolished the effects of miR-361-3p upregulation in H1299/DDP and A549/DDP cells (Figure 6(b)–(i)). These results

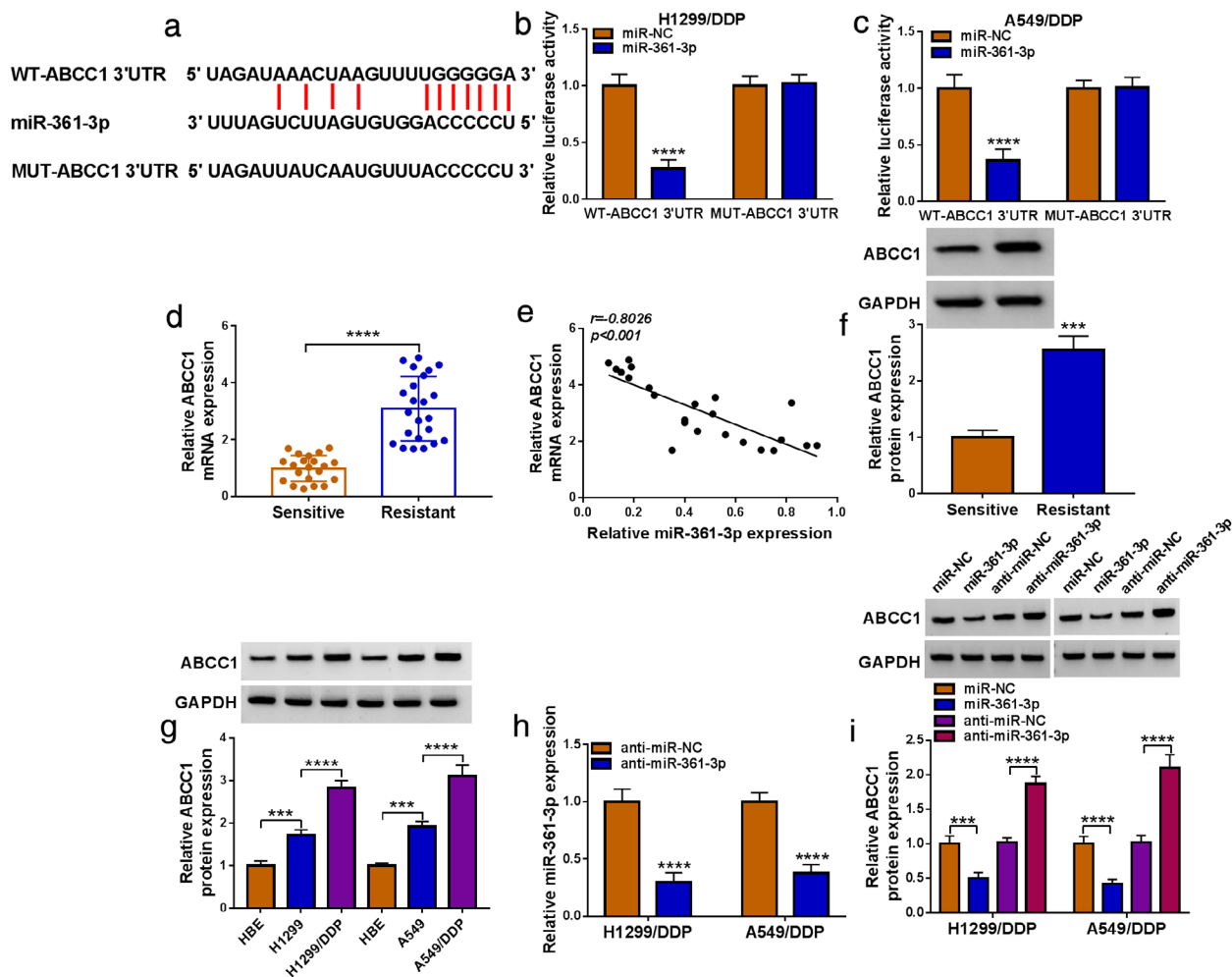


FIGURE 5 MiR-361-3p direct targets and inhibits ABCC1. (a) Sequence of miR-361-3p, the putative miR-361-3p complementary sequence within ABCC1 3'UTR and the mutation in the target sequence. (b) and (c) Dual-luciferase reporter assay revealing the repression of miR-361-3p on the luciferase activity of the wild-type 3'UTR reporter construct (WT-ABCC1 3'UTR), but not mutant reporter construct (MUT-ABCC1 3'UTR). (d) qRT-PCR analysis of ABCC1 mRNA expression in clinical NSCLC tissues from 23 recurrent patients after treatment of DDP-based chemotherapy (Resistant) and 21 primary patients before therapeutic treatment (Sensitive). (e) Expression analysis of ABCC1 mRNA and miR-361-3p in NSCLC tissues from 23 recurrent patients after treatment of DDP-based chemotherapy (Resistant). (f) Western blot of ABCC1 protein level in clinical NSCLC tissues from five recurrent patients after treatment of DDP-based chemotherapy (Resistant) and five primary patients before therapeutic treatment (Sensitive). (g) Western blot of ABCC1 protein level in A549/DDP, A549, H1299/DDP, H1299 NSCLC cells and human normal HBE cells. (h) qRT-PCR analysis of miR-361-3p expression in anti-miR-NC- or anti-miR-361-3p-transfected H1299/DDP and A549/DDP cells. (i) Relative ABCC1 protein level by western blot in H1299/DDP and A549/DDP cells introduced with anti-miR-361-3p, anti-miR-NC, miR-361-3p mimic or miR-NC mimic. *** $p < 0.001$, **** $p < 0.0001$

collectively establish the notion that miR-361-3p affects the functional properties of H1299/DDP and A549/DDP cells at least in part by targeting ABCC1.

Circ_0058357 operates as a regulator of ABCC1 expression through miR-361-3p

The above observations demonstrated that circ_0058357 and ABCC1 harbor a shared binding sequence for miR-361-3p. Hence, we next decided to investigate whether circ_0058357 could affect ABCC1 expression. Indeed, ABCC1 protein level was remarkably reduced in circ_0058357-silenced H1299/DDP and A549/DDP cells; however, this effect was strongly abated by miR-361-3p downregulation (Figure 7(a),(b)). All

these findings suggest that circ_0058357 affects ABCC1 expression by competitively binding to shared miR-361-3p.

Inhibition of circ_0058357 diminishes the growth of A549/DDP cells and sensitizes them to the cytotoxic effect of DDP in vivo

To determine whether circ_0058357 possesses regulatory effects in vivo, we transduced A549/DDP cells with sh-circ_0058357 or sh-NC and injected them subcutaneously into the right flanks of BALB/c nude mice before DDP or PBS administration. Strikingly, sh-circ_0058357 transduction or DDP administration repressed tumor growth (Figure 8(a),(b)). Interestingly, simultaneous sh-circ_0058357 transduction and

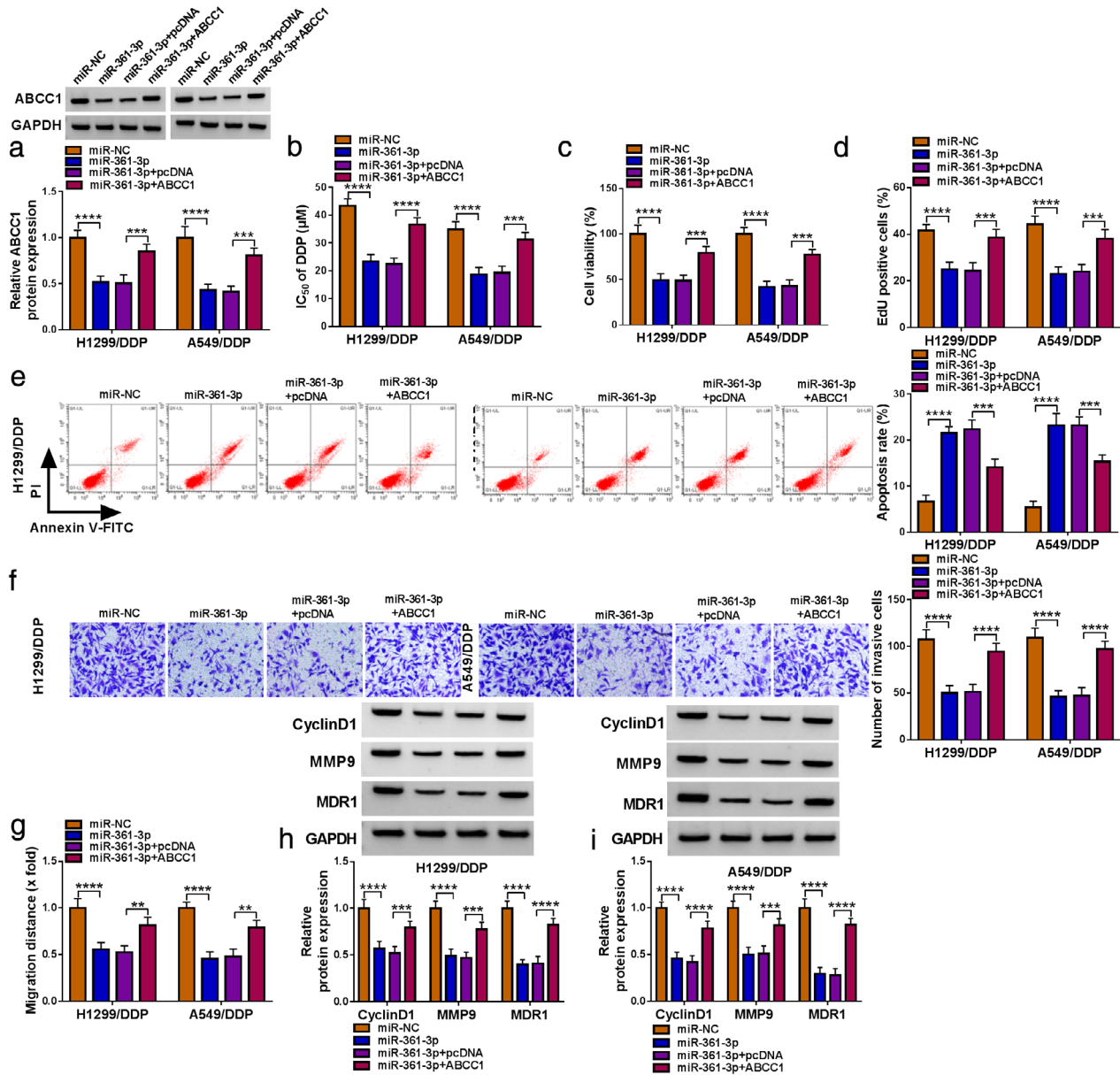


FIGURE 6 ABCC1 is a functional target of miR-361-3p. (a)–(i) H1299/DDP and A549/DDP cells were transfected with miR-361-3p mimic+ABCC1 expression plasmid, miR-361-3p mimic+pcDNA control plasmid, miR-361-3p mimic or miR-NC mimic. (a) Western blot showing ABCC1 protein level in transfected H1299/DDP and A549/DDP cells. (b) Transfected H1299/DDP and A549/DDP cells were exposed to various concentrations of DDP and checked for cell survival and the IC₅₀ value by MTT assay. (c) MTT assay for the viability of transfected H1299/DDP and A549/DDP cells. (d) EdU assay for the proliferation of transfected H1299/DDP and A549/DDP cells. (e) Cell apoptosis of transfected H1299/DDP and A549/DDP cells by flow cytometry. (f) Cell invasion of transfected H1299/DDP and A549/DDP cells by transwell assay. (g) Cell migration of transfected H1299/DDP and A549/DDP cells by wound-healing assay. (h) and (i) Western blot showing CyclinD1, MMP9 and MDR1 levels in transfected H1299/DDP and A549/DDP cells. ***p* < 0.01, ****p* < 0.001, *****p* < 0.0001

DDP administration led to a clearer repression in tumor growth (Figure 8(a),(b)). Furthermore, sh-circ_0058357-transduced tumors showed reduced levels of circ_0058357 and ABCC1 protein and increased expression of miR-361-3p with or without DDP administration (Figure 8(c)–(e)). Our immunohistochemistry analysis also showed a strong reduction in the level of metastasis-related MMP9 protein^{23,24} in sh-circ_0058357-transduced tumors with or without DDP administration (Figure 8(e)), suggesting that circ_0058357 depletion may weaken the metastatic potential of the tumors.

All these data suggest that downregulation of circ_0058357 expression diminishes tumor growth and enhances DDP sensitivity in vivo.

DISCUSSION

Drug resistance has become a major reason behind the failure of chemotherapy in NSCLC.²⁵ However, little is known about DDP resistance mechanisms. Intense efforts have led

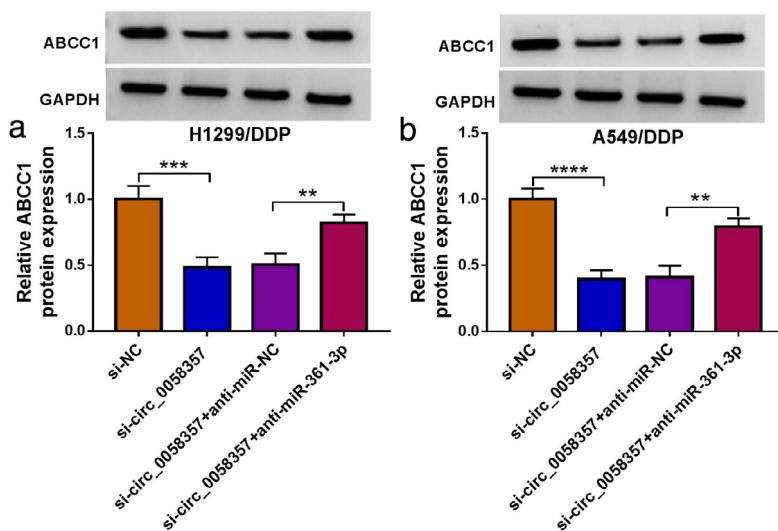


FIGURE 7 Circ_0058357 affects ABCC1 expression through miR-361-3p. H1299/DDP (a) and A549/DDP (b) cells were transfected with si-circ_0058357 + anti-miR-361-3p, si-circ_0058357 + anti-miR-NC, si-circ_0058357 or si-NC and checked for ABCC1 protein level by western blot. ** $p < 0.01$, *** $p < 0.001$, **** $p < 0.0001$

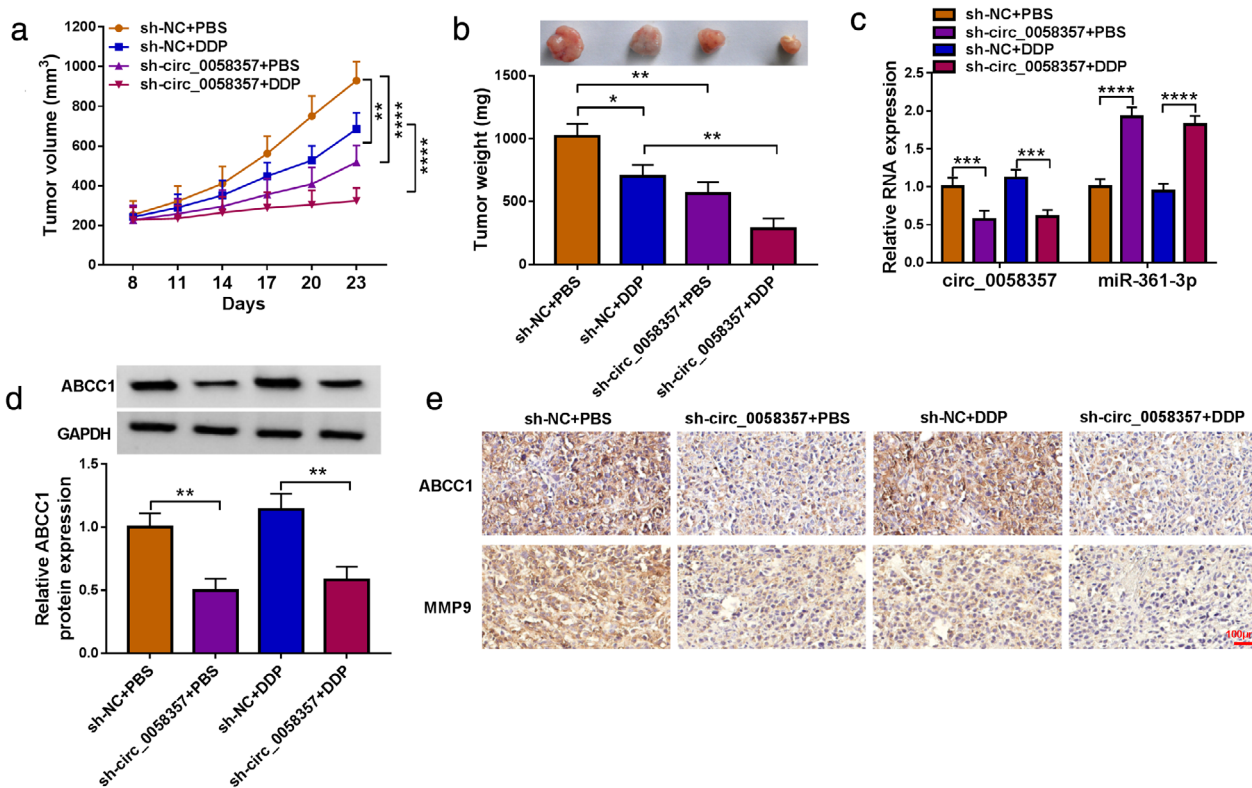


FIGURE 8 Inhibition of circ_0058357 represses tumor growth and sensitizes A549/DDP cells to DDP in vivo. (a)–(e) A549/DDP cells infected with sh-circ_0058357 or sh-NC were injected (4×10^6 cells each mouse) subcutaneously into BALB/c nude mice. After eight days, DDP (30 mg/kg, every 3 days) or PBS administration and tumor volume measurement began. Each group included six mice. Twenty-three days later, tumors were collected. (a) Growth curve of the tumors. (b) Representative images and mean weight of the xenograft tumors. (c) qRT-PCR analysis of circ_0058357 and miR-361-3p levels in the tumors. (d) Western blot showing ABCC1 protein level in the excised tumors. (e) Immunohistochemistry of ABCC1 and MMP9 protein levels in the tumors. Scale bar: 100 μm . * $p < 0.05$, ** $p < 0.01$, *** $p < 0.001$, **** $p < 0.0001$

to the identification of deregulated circRNA activity in the development of DDP resistance in NSCLC.^{8,10,26} In this study, we have demonstrated the influence of circ_0058357 on the functional properties and DDP sensitivity of H1299/DDP and A549/DDP cells. More importantly, we have

established a new circRNA/miRNA/mRNA network implicated in the regulation of DDP-resistant NSCLC cells.

Our findings showed the overexpression of circ_0058357 in DDP-resistant NSCLC. Consistent with the recent work showing the tumor-inhibitory effect of circ_0058357

deficiency on NSCLC,¹² we first demonstrated that inhibition of circ_0058357 impedes the growth and metastasis of H1299/DDP and A549/DDP cells and sensitizes them to the cytotoxic effects of DDP. As previously reported for other circRNAs,^{27,28} circ_0058357 is RNase R resistant because of its covalently bonded structure.⁴ Additionally, the cytoplasmic localization of circ_0058357 in H1299/DDP and A549/DDP cells provides the possibility for the interactions between circ_0058357 and miRNAs because miRNAs silence gene expression in the cytoplasm in the RNA-induced silencing complex (RISC).²⁹

Numerous circRNAs form a crucial type of post-transcriptional regulators by inhibiting miRNA activity.³⁰ Here, we first ascertained that circ_0058357 harbors a miR-361-3p binding site, and the effects of circ_0058357 inhibition are partially due to the elevation of miR-361-3p. The dual role of miR-361-3p in human carcinogenesis as either tumor inhibitors or tumor drivers has been highlighted (for instance): miR-361-3p contributes to the development of pancreatic cancer³¹ and breast cancer³²; miR-361-3p works as a strong anticancer factor in lymphoma³³ and ovarian cancer.³⁴ The contradictory findings may be attributed to the different types of tumors in these reports. In line with previous studies showing the anticancer activity of miR-361-3p in NSCLC,^{14–16} we uncovered that miR-361-3p hinders the growth and metastasis of H1299/DDP and A549/DDP cells and sensitizes them to DDP therapy. A recent study has also discovered that miR-361-3p can promote enzalutamide (Enz) sensitivity of Enz-resistant prostate cancer by targeting androgen receptor splicing variant 7 (ARv7).³⁵

ABCC1 participates in the development of drug resistance in cancers, such as hepatocellular, colon and ovarian cancers.^{36–38} Moreover, ABCC1 exerts an important promoting effect on the development of DDP resistance in NSCLC.^{19–21} In this study, we first showed that miR-361-3p inhibits ABCC1 expression through the perfect binding sequence in ABCC1 3'UTR, and inhibition of ABCC1 by miR-361-3p is partially responsible for the regulation of miR-361-3p in the growth, metastasis and DDP sensitivity of H1299/DDP and A549/DDP cells. Pei et al.²¹ reported that miR-185-5p affected DDP sensitivity of NSCLC by targeting ABCC1. Furthermore, we pointed to the role of circ_0058357 as a post-transcriptional regulator of ABCC1 expression by competing for binding to miR-361-3p. ABC efflux transporters, including ABCC1, contribute to drug resistance in cancer cells by limiting the exposure to anticancer drugs.³⁹ Thus, developing the inhibitors of ABC efflux transporters is an effective approach to overcome drug resistance. With our findings, we envision that inhibition of circ_0058357 may be a promising point for the development of circRNA-based therapies against DDP resistance in NSCLC.

Taken together, we have demonstrated that inhibition of circ_0058357 suppresses the growth and metastasis of H1299/DDP and A549/DDP cells and sensitizes them to DDP therapy. We have identified a novel circ_0058357/miR-361-3p/ABCC1 network which regulates the DDP resistance of NSCLC.

CONFLICT OF INTEREST

The authors report no conflicts of interest.

ORCID

Pengfei Jiao  <https://orcid.org/0000-0003-2379-6534>

REFERENCES

- Bray F, Ferlay J, Soerjomataram I, Siegel RL, Torre LA, Jemal A. Global cancer statistics 2018: GLOBOCAN estimates of incidence and mortality worldwide for 36 cancers in 185 countries. *CA Cancer J Clin.* 2018;68:394–424.
- Herbst RS, Morgensztern D, Boshoff C. The biology and management of non-small cell lung cancer. *Nature.* 2018;553:446–54.
- Rossi A, Di Maio M. Platinum-based chemotherapy in advanced non-small-cell lung cancer: optimal number of treatment cycles. *Expert Rev Anticancer Ther.* 2016;16:653–60.
- Kristensen LS, Andersen MS, Stagsted LVW, Ebbesen KK, Hansen TB, Kjems J. The biogenesis, biology and characterization of circular RNAs. *Nat Rev Genet.* 2019;20:675–91.
- Tay Y, Rinn J, Pandolfi PP. The multilayered complexity of ceRNA crosstalk and competition. *Nature.* 2014;505:344–52.
- Anastasiadou E, Jacob LS, Slack FJ. Non-coding RNA networks in cancer. *Nat Rev Cancer.* 2018;18:5–18.
- Xu T, Wang M, Jiang L, Ma L, Wan L, Chen Q, et al. CircRNAs in anticancer drug resistance: recent advances and future potential. *Mol Cancer.* 2020;19:127.
- Song L, Cui Z, Guo X. Comprehensive analysis of circular RNA expression profiles in cisplatin-resistant non-small cell lung cancer cell lines. *Acta Biochim Biophys Sin (Shanghai).* 2020;52:944–53.
- Lu H, Xie X, Wang K, Chen Q, Cai S, Liu D, et al. Circular RNA hsa_circ_0096157 contributes to cisplatin resistance by proliferation, cell cycle progression, and suppressing apoptosis of non-small-cell lung carcinoma cells. *Mol Cell Biochem.* 2020;475:63–77.
- Pang J, Ye L, Zhao D, Zhao D, Chen Q. Circular RNA PRMT5 confers cisplatin-resistance via miR-4458/REV3L axis in non-small-cell lung cancer. *Cell Biol Int.* 2020;44:2416–26.
- Zhong Y, Lin H, Li Q, Liu C, Shen J. CircRNA_100565 contributes to cisplatin resistance of NSCLC cells by regulating proliferation, apoptosis and autophagy via miR-337-3p/ADAM28 axis. *Cancer Biomark.* 2021;30:261–73.
- Wei D, Sun L, Feng W. hsa_circ_0058357 acts as a ceRNA to promote non-small cell lung cancer progression via the hsa-miR-24-3p/AVL9 axis. *Mol Med Rep.* 2021;23:470.
- Wang Q, Zhong M, Liu W, Li J, Huang J, Zheng L. Alterations of microRNAs in cisplatin-resistant human non-small cell lung cancer cells (A549/DDP). *Exp Lung Res.* 2011;37:427–34.
- Chen W, Wang J, Liu S, Wang S, Cheng Y, Zhou W, et al. MicroRNA-361-3p suppresses tumor cell proliferation and metastasis by directly targeting SH2B1 in NSCLC. *J Exp Clin Cancer Res.* 2016;35:76.
- Li X, Zheng H. LncRNA SNHG1 influences cell proliferation, migration, invasion, and apoptosis of non-small cell lung cancer cells via the miR-361-3p/FRAT1 axis. *Thorac Cancer.* 2020;11:295–304.
- Chen L, Nan A, Zhang N, Jia Y, Li X, Ling Y, et al. Circular RNA 100146 functions as an oncogene through direct binding to miR-361-3p and miR-615-5p in non-small cell lung cancer. *Mol Cancer.* 2019;18:13.
- Ma W, Kang Y, Ning L, Tan J, Wang H, Ying Y. Identification of microRNAs involved in gefitinib resistance of non-small-cell lung cancer through the insulin-like growth factor receptor 1 signaling pathway. *Exp Ther Med.* 2017;14:2853–62.
- Robey RW, Pluchino KM, Hall MD, Fojo AT, Bates SE, Gottesman MM. Revisiting the role of ABC transporters in multidrug-resistant cancer. *Nat Rev Cancer.* 2018;18:452–64.
- Fan CC, Tsai ST, Lin CY, Chang LC, Yang JC, Chen GY, et al. EFHD2 contributes to non-small cell lung cancer cisplatin resistance by the activation of NOX4-ROS-ABCC1 axis. *Redox Biol.* 2020;34:101571.

20. Wang Q, Geng F, Zhou H, Chen Y, Du J, Zhang X, et al. MDIG promotes cisplatin resistance of lung adenocarcinoma by regulating ABC transporter expression via activation of the WNT/ β -catenin signaling pathway. *Oncol Lett.* 2019;18:4294–307.
21. Pei K, Zhu JJ, Wang CE, Xie QL, Guo JY. MicroRNA-185-5p modulates chemosensitivity of human non-small cell lung cancer to cisplatin via targeting ABCC1. *Eur Rev Med Pharmacol Sci.* 2016;20:4697–704.
22. Hatley ME, Patrick DM, Garcia MR, Richardson JA, Bassel-Duby R, van Rooij E, et al. Modulation of K-Ras-dependent lung tumorigenesis by MicroRNA-21. *Cancer Cell.* 2010;18:282–93.
23. Gu JJ, Hoj J, Rouse C, Pendergast AM. Mesenchymal stem cells promote metastasis through activation of an ABL-MMP9 signaling axis in lung cancer cells. *PLoS One.* 2020;15:e0241423.
24. Li J, Wang H, Ke H, Ni S. MiR-129 regulates MMP9 to control metastasis of non-small cell lung cancer. *Tumour Biol.* 2015;36:5785–90.
25. Terlizzi M, Colarusso C, Pinto A, Sorrentino R. Drug resistance in non-small cell lung Cancer (NSCLC): impact of genetic and non-genetic alterations on therapeutic regimen and responsiveness. *Pharmacol Ther.* 2019;202:140–8.
26. Zhao Y, Zheng R, Chen J, Ning D. CircRNA CDR1as/miR-641/HOXA9 pathway regulated stemness contributes to cisplatin resistance in non-small cell lung cancer (NSCLC). *Cancer Cell Int.* 2020;20:289.
27. Pan Z, Cai J, Lin J, Zhou H, Peng J, Liang J, et al. A novel protein encoded by circFNDC3B inhibits tumor progression and EMT through regulating Snail in colon cancer. *Mol Cancer.* 2020;19:71.
28. Li M, Ding W, Tariq MA, Chang W, Zhang X, Xu W, et al. A circular transcript of ncx1 gene mediates ischemic myocardial injury by targeting miR-133a-3p. *Theranostics.* 2018;8:5855–69.
29. Iwakawa HO, Tomari Y. The functions of MicroRNAs: mRNA decay and translational repression. *Trends Cell Biol.* 2015;25:651–65.
30. Memczak S, Jens M, Elefsinioti A, Torti F, Krueger J, Rybak A, et al. Circular RNAs are a large class of animal RNAs with regulatory potency. *Nature.* 2013;495:333–8.
31. Hu J, Li L, Chen H, Zhang G, Liu H, Kong R, et al. MiR-361-3p regulates ERK1/2-induced EMT via DUSP2 mRNA degradation in pancreatic ductal adenocarcinoma. *Cell Death Dis.* 2018;9:807.
32. Hua B, Li Y, Yang X, Niu X, Zhao Y, Zhu X. MicroRNA-361-3p promotes human breast cancer cell viability by inhibiting the E2F1/P73 signalling pathway. *Biomed Pharmacother.* 2020;125:109994.
33. Zhou H, Tang H, Li N, Chen H, Chen X, Gu L, et al. MicroRNA-361-3p inhibit the progression of lymphoma by the Wnt/ β -catenin signaling pathway. *Cancer Manag Res.* 2020;12:12375–84.
34. Yao H, Chen R, Yang Y, Jiang J. LncRNA BBOX1-AS1 aggravates the development of ovarian cancer by sequestering miR-361-3p to augment PODXL expression. *Reprod Sci.* 2021;28:736–44.
35. Liu B, Sun Y, Tang M, Liang C, Huang CP, Niu Y, et al. The miR-361-3p increases enzalutamide (Enz) sensitivity via targeting the ARv7 and MKNK2 to better suppress the Enz-resistant prostate cancer. *Cell Death Dis.* 2020;11:807.
36. Huang H, Chen J, Ding CM, Jin X, Jia ZM, Peng J. LncRNA NR2F1-AS1 regulates hepatocellular carcinoma oxaliplatin resistance by targeting ABCC1 via miR-363. *J Cell Mol Med.* 2018;22:3238–45.
37. Lin H, Yang G, Yu J, Wang J, Li Q, Guo S, et al. KDM5c inhibits multidrug resistance of colon cancer cell line by down-regulating ABCC1. *Biomed Pharmacother.* 2018;107:1205–9.
38. Zhou S, Wang R, Xiao H. Adipocytes induce the resistance of ovarian cancer to carboplatin through ANGPTL4. *Oncol Rep.* 2020;44:927–38.
39. Choi YH, Yu AM. ABC transporters in multidrug resistance and pharmacokinetics, and strategies for drug development. *Curr Pharm Des.* 2014;20:793–807.

SUPPORTING INFORMATION

Additional supporting information may be found in the online version of the article at the publisher's website.

How to cite this article: Chu D, Li P, Li Y, Shi J, Huang S, Jiao P. Identification of circ_0058357 as a regulator in non-small cell lung cancer cells resistant to cisplatin by miR-361-3p/ABCC1 axis. *Thorac Cancer.* 2021;12:2894–906. <https://doi.org/10.1111/1759-7714.14150>